The structure of phosphate glass biomaterials from neutron diffraction and ^{31}P nuclear magnetic resonance data

2007 J. Phys.: Condens. Matter 19 415116

(http://iopscience.iop.org/0953-8984/19/41/415116)

IOP PUBLISHING JOURNAL OF PHYSICS: CONDENSED MATTER

J. Phys.: Condens. Matter **19** (2007) 415116 (8pp) doi:10.1088/0953-8984/19/41/415116

The structure of phosphate glass biomaterials from neutron diffraction and ^{31}P nuclear magnetic resonance data

D M Pickup[1], **I Ahmed**[2], **P Guerry**[3], **J C Knowles**[2], **M E Smith**[3] **and R J Newport**[1]

[1] School of Physical Sciences, University of Kent, Canterbury CT2 7NH, UK
[2] Division of Biomaterials and Tissue Engineering, UCL Eastman Dental Institute, 256 Gray's Inn Road, London WC1X 8LD, UK
[3] Department of Physics, University of Warwick, Coventry CV4 7AL, UK

Received 6 March 2007, in final form 11 April 2007
Published 27 September 2007
Online at stacks.iop.org/JPhysCM/19/415116

Abstract
Neutron diffraction and ^{31}P nuclear magnetic resonance spectroscopy were used to probe the structure of phosphate glass biomaterials of general composition $(CaO)_{0.5-x}(Na_2O)_x(P_2O_5)_{0.5}$ ($x = 0$, 0.1 and 0.5). The results suggest that all three glasses have structures based on chains of Q^2 phosphate groups. Clear structural differences are observed between the glasses containing Na_2O and CaO. The P–O bonds to bridging and non-bridging oxygens are less well resolved in the neutron data from the samples containing CaO, suggesting a change in the nature of the bonding as the field strength of the cation increases $Na^+ \rightarrow Ca^{2+}$. In the $(CaO)_{0.5}(P_2O_5)_{0.5}$ glass most of the Ca^{2+} ions are present in isolated CaO_x polyhedra whereas in the $(Na_2O)_{0.5}(P_2O_5)_{0.5}$ glass the NaO_x polyhedra share edges leading to a Na–Na correlation. The results of the structural study are related to the properties of the $(CaO)_{0.4}(Na_2O)_{0.1}(P_2O_5)_{0.5}$ biomaterial.

1. Introduction

The general trend in biomaterials research is a move from passive, inert implant materials to those that degrade and play an active part in the regeneration of tissue [1]. A greater understanding of the interaction of materials with cells has allowed implant materials to be designed with the aim of promoting a specific biological response. This new class of materials is often referred to as the 'Third Generation' of biomaterials, and included in this class are biocompatible phosphate glasses.

Phosphate based glasses have many unique properties, the most interesting of which, from a biomedical standpoint, is their ability to dissolve completely in aqueous media. Furthermore, this dissolution behaviour may be easily controlled via the chemistry of the glasses [2]. Of benefit to biomedical applications is the fact that these glasses can be prepared to include ions routinely found in the human body. Because of these properties, phosphate based glasses can find application as degradable temporary implants in the human body: reacting and dissolving in the physiological environment, and eventually being replaced by hard or soft tissue.

Further to the properties described above, phosphate based glasses can also have a beneficial effect on cell proliferation. Bitar *et al* [3] demonstrated that ternary phosphate glasses with high calcium content can support the attachment, growth and differentiation of human osteoblasts and fibroblasts. Consequently, there has been significant interest in these glasses when manufactured as fibres for potential use in tissue engineering, and in particular, for any tissue with a medium to high anisotropy, such as muscle and ligament [4]. Other potential clinical applications of phosphate based glasses include bacterial control devices when doped with antibacterial ions, as neural repair devices when manufactured in a tubular form and as a component in oral healthcare products when doped with fluoride ions [1].

Whilst significant work has been carried out to elucidate the structure of phosphate glasses [5], there is a scarcity of data to correlate this information with the physical properties such as dissolution rate. In this paper, we have studied the structure of phosphate glass biomaterials of general composition $(CaO)_{0.5-x}(Na_2O)_x(P_2O_5)_{0.5}$ with neutron diffraction and ^{31}P NMR spectroscopy in order to better understand the structure/properties relationship.

2. Experimental: preparation of the phosphate glasses

The phosphate glasses were prepared using sodium dihydrogen orthophosphate (NaH_2PO_4, 99%, BDH), calcium carbonate ($CaCO_3$, 99 + %, BDH) and phosphorus pentoxide (P_2O_5, 97%, BDH). The precursors were weighed out, mixed, placed in a Pt/10%Rh crucible (Type 71040, Johnson Matthey) and loaded into a preheated furnace (Carbolite, RHF 1500, UK). The mixture was left at 300 °C for half an hour, raised to 600 °C for a further half an hour and finally melted at 1100 °C for 1 h. The molten glass was then poured into a preheated (370 °C) graphite mould, and left to cool to room temperature.

Characterization necessary for analysis of the neutron diffraction data was performed: elemental analysis (ICP-AES and gravimetric) was carried out by a commercial company (Medac Ltd) and macroscopic densities were determined by helium pycnometry using a Quantachrome Multipycnometer. The experimentally determined compositions were found to agree with the expected values within experimental error.

3. Experimental: structural studies

The neutron diffraction data presented here were collected on the GEM diffractometer on the ISIS spallation neutron source at the Rutherford Appleton Laboratory, UK. The samples were in the form of 8 mm diameter rods, which negated the need for a container (thus simplifying the necessary corrections to the data), and time-of-flight data collected over a wide range of Q (up to 60 Å^{-1}, where $Q = 4\pi \sin\theta/\lambda$). The program GUDRUN was used to reduce and correct the data [6].

The initial stage of analysis of diffraction data from an amorphous material involves the removal of background scattering, normalization, correction for absorption, inelastic and multiple scattering and subtraction of the self-scattering term [6]. The resultant scattered intensity, $i(Q)$, can reveal structural information by Fourier transformation to obtain the pair distribution function:

$$T(r) = T^0(r) + \frac{2}{\pi}\int_0^\infty Qi(Q)M(Q)\sin(Qr)\,\mathrm{d}Q \qquad (1)$$

where $T^0(r) = 4\pi r\rho^0\bar{b}^2$ is the average density contribution (r is the atomic separation between atoms, ρ^0 the macroscopic number density and $\bar{b}$ is the average coherent scattering length) and $M(Q)$ is a window function necessitated by the finite maximum experimentally attainable value of Q.

Structural information can be obtained from the diffraction data by simulating the Q-space data and converting the results to r-space by Fourier transformation to allow comparison with the experimentally determined correlation function [7]. The Q-space simulation is generated using the following equation:

$$p(Q)_{ij} = \frac{N_{ij}w_{ij}}{c_j}\frac{\sin QR_{ij}}{QR_{ij}}\exp\left[\frac{-Q^2\sigma_{ij}^2}{2}\right] \tag{2}$$

where $p(Q)_{ij}$ is the pair function in reciprocal space, N_{ij}, R_{ij} and σ_{ij} are the coordination number, atomic separation and disorder parameter, respectively, of atom i with respect to j, c_j is the concentration of atom j and w_{ij} is the weighting factor, given by:

$$w_{ij} = 2c_ic_jb_ib_j \qquad \text{if } i \neq j \tag{3}$$

or,

$$w_{ij} = c_i^2b_i^2 \qquad \text{if } i = j \tag{4}$$

where b represents the coherent scattering length.

The ^{31}P NMR experiments were carried out on a CMX Infinity spectrometer attached to an 8.5 T magnet giving a ^{31}P Larmor frequency of 145.85 MHz. Samples were placed in the magnet using a Doty 4 mm MAS (magic angle spinning) probe and spun at ~12 kHz. Spectra were recorded using the Spinsight software running a simple one (90°) pulse experiment. The 90° pulse length was 2 μs. A repetition time of 30 s was chosen to avoid saturation. Typically, 70 scans were accumulated to obtain an adequate signal/noise ratio. Spectra were referenced to the resonance of $NH_4H_2PO_4$ at 0.9 ppm.

4. Results

Figures 1, 2 and 3 show the neutron diffraction data from the $(CaO)_{0.5}(P_2O_5)_{0.5}$, $(Na_2O)_{0.5}(P_2O_5)_{0.5}$ and $(CaO)_{0.4}(Na_2O)_{0.1}(P_2O_5)_{0.5}$ glasses, respectively. Both the r-space and Q-space data are shown, together with the fits to the pair distributions functions obtained using the method described above. The structural parameters obtained from the fitting of the neutron diffraction data are given in table 1. The peak assignments used in the fitting process were taken from the literature reports of previous work on phosphate glass containing CaO and Na_2O [5]. The strongest peaks in the pair distributions functions at ~1.5 Å and ~2.5 Å are due to the P–O and O–O nearest-neighbour distances, respectively. The shoulder to the low r side of the O–O peak is the metal–oxygen correlation and the shoulder at ~3 Å is due to the shortest P–P distance in the structure. The second nearest-neighbour oxygen–oxygen distance ($O\text{–}O_{2nd}$) was taken from an x-ray diffraction study of vitreous P_2O_5 (v-P_2O_5) [8].

Figure 4 shows the ^{31}P MAS NMR spectra from the $(Na_2O)_{0.5}(P_2O_5)_{0.5}$, $(CaO)_{0.5}(P_2O_5)_{0.5}$ and $(CaO)_{0.4}(Na_2O)_{0.1}(P_2O_5)_{0.5}$ samples. For the $(CaO)_{0.5}(P_2O_5)_{0.5}$ sample, two peaks are present at −10.4 ppm and −27.4 ppm. These are ascribed to Q^1 and Q^2 structural units, where n in Q^n refers to the number of bridging oxygen atoms in the PO_4^{3-} structural unit (and hence the number of other PO_4^{3-} groups connected to it). Fitting of the spectrum revealed the presence of 96% Q^2 and 4% Q^1. The chemical shifts (−10.4 ppm for Q^1 and −27.4 ppm for Q^2) agree with previously published results [9]. The spectrum from the $(CaO)_{0.4}(Na_2O)_{0.1}(P_2O_5)_{0.5}$ glass is almost identical to that from the $(CaO)_{0.5}(P_2O_5)_{0.5}$ sample. The spectrum from the $(Na_2O)_{0.5}(P_2O_5)_{0.5}$ sample shows only the presence of Q^2 with a peak at −19.8 ppm, in agreement with previously published work [5].

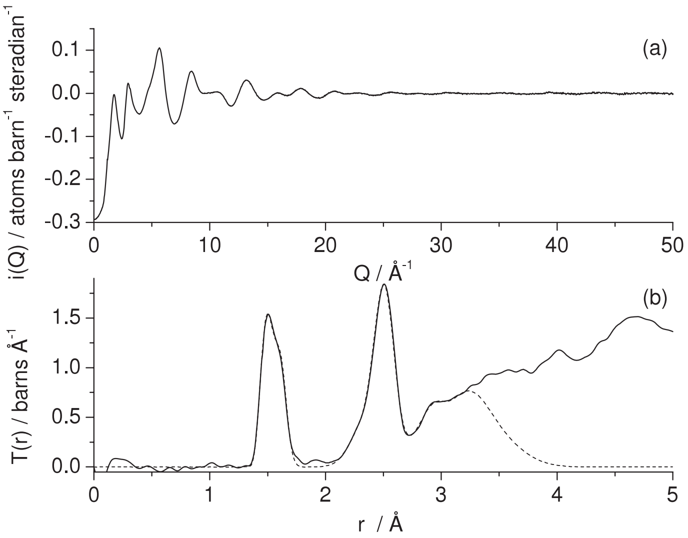

Figure 1. Neutron diffraction data from the $(CaO)_{0.5}(P_2O_5)_{0.5}$ glass: (a) Q-space interference function, $i(Q)$, and (b) pair distribution function, $T(r)$, (solid line) together with fit (dashed line).

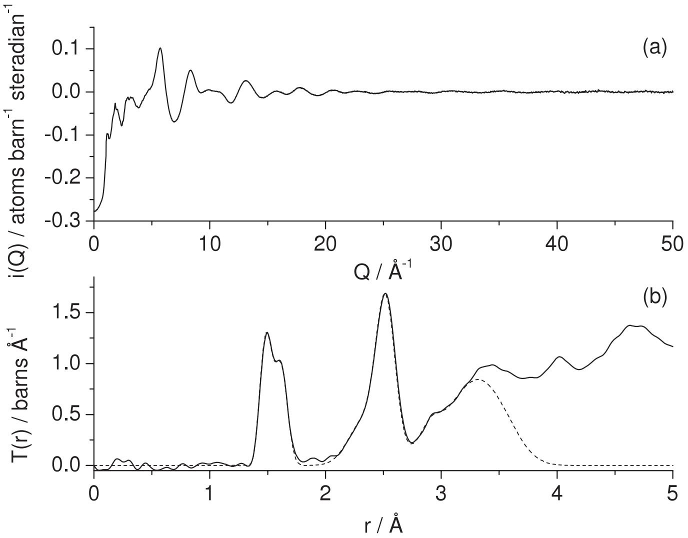

Figure 2. Neutron diffraction data from the $(Na_2O)_{0.5}(P_2O_5)_{0.5}$ glass: (a) Q-space interference function, $i(Q)$, and (b) pair distribution function, $T(r)$, (solid line) together with fit (dashed line).

5. Discussion

It is well known that the building blocks of phosphate based glasses are PO_4^{3-} tetrahedra [5]. Each PO_4^{3-} can be connected to a maximum of three other such units to form a three-dimensional network, as in v-P_2O_5. Additions of metal oxides cause the connectivity of the PO_4^{3-} groups to be reduced and chain-like structures or structures containing isolated phosphate anions are formed. Two P–O distances may be observed in phosphate glasses: a shorter

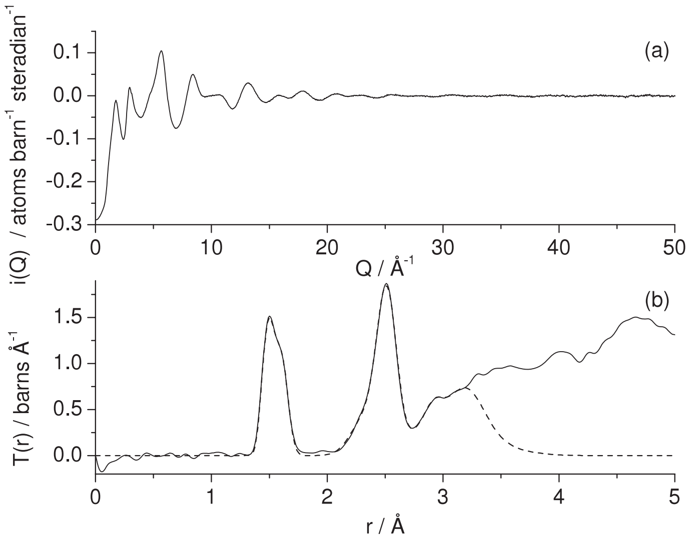

Figure 3. Neutron diffraction data from the $(CaO)_{0.4}(Na_2O)_{0.1}(P_2O_5)_{0.5}$ glass: (a) Q-space interference function, $i(Q)$, and (b) pair distribution function, $T(r)$, (solid line) together with fit (dashed line).

Table 1. Structural parameters obtained from the simulations of the neutron diffraction data. Note that reasonable estimates of the errors are ±0.02 Å in R, ±15% in N and ±0.010 Å in σ.

Sample	Density (g cm^{-3})	Correlation	R (Å)	N	σ (Å)
$(CaO)_{0.5}(P_2O_5)_{0.5}$	2.61	P–NBO	1.49	1.9	0.034
		P–BO	1.60	2.0	0.046
		Ca–O	2.34	4.9	0.120
		O–O	2.51	4.0	0.080
		P–P	2.94	1.9	0.078
		O–O$_{2nd}$	2.82	0.9	0.115
$(Na_2O)_{0.5}(P_2O_5)_{0.5}$	2.47	P–NBO	1.48	1.8	0.034
		P–BO	1.61	2.0	0.048
		Na–O	2.33	4.0	0.130
		O–O	2.52	4.0	0.078
		P–P	2.93	2.0	0.070
		Na–Na	3.07	1.4	0.080
		O–O$_{2nd}$	2.82	0.6	0.100
$(CaO)_{0.4}(Na_2O)_{0.1}(P_2O_5)_{0.5}$	2.59	P–NBO	1.49	1.9	0.036
		P–BO	1.60	2.0	0.048
		Na–O	2.33	3.5	0.130
		Ca–O	2.34	4.9	0.120
		O–O	2.52	4.2	0.080
		P–P	2.93	2.1	0.070
		O–O$_{2nd}$	2.82	1.0	0.115

distance of ~1.49 Å ascribed to bonds to non-bridging oxygens (NBOs) and a longer distance of ~1.60 Å due to bonds to bridging oxygens (BOs).

The results in table 1 indicate that, in the glasses studied here, the number of NBOs and BOs connected to each phosphorus atom are equal. This is to be expected from the composition

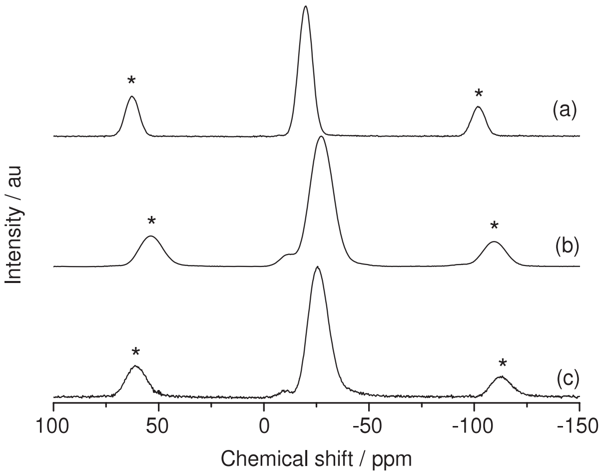

Figure 4. ^{31}P MAS NMR spectra: (a) $(Na_2O)_{0.5}(P_2O_5)_{0.5}$, (b) $(CaO)_{0.5}(P_2O_5)_{0.5}$ and (c) $(CaO)_{0.4}(Na_2O)_{0.1}(P_2O_5)_{0.5}$ glasses.

of the glasses. If it is assumed that all the phosphorus atoms are bonded to four oxygens, and that all the oxygens are bonded to either one or two P atoms then the P–NBO coordination number is:

$$n_{\mathrm{P-NBO}} = 2\frac{N_{\mathrm{O}}}{N_{\mathrm{P}}} - 4 \tag{5}$$

and similarly the P–BO coordination number is:

$$n_{\mathrm{P-BO}} = 8 - 2\frac{N_{\mathrm{O}}}{N_{\mathrm{P}}} \tag{6}$$

where N_{O} and N_{P} are the numbers of oxygen and phosphorus atoms in the sample. The samples studied here are predicted to have coordination numbers of two for both the P–O first-shell correlations, in agreement (within the errors associated with the measurements) with the experimental results from the neutron diffraction study. This result is supported by the analysis of the ^{31}P MAS NMR spectra. PO_4^{3-} groups with two NBOs and two BOs correspond to Q^2 units in the NMR terminology. The NMR results suggest structures based on Q^2 units. The small amount of Q^1 (<5%) observed in the Ca containing samples is likely to be due to partial hydrolysis of the structure which is known to occur in phosphate glasses [5]. The P–P coordination numbers of close to two for all three glass samples also provide evidence for structures based on chains of Q^2 groups.

Of particular interest in relation to understanding the properties of $(CaO)_{0.5-x}(Na_2O)_x(P_2O_5)_{0.5}$ glasses is the effect the cations have on the phosphate skeleton that forms the basis of the structure. With regard to this, it is useful to consider the ratio of NBOs per Me^{v+} cation, $\mathrm{M_{NBO}}$, which is given by [10]:

$$\mathrm{M_{NBO}} = N_{\mathrm{NBO}}/N_{\mathrm{Me}} = v(y+1)/y \tag{7}$$

where N_{NBO} and N_{Me} are the numbers of NBOs and cations, respectively, and y is the molar ratio of metal oxide to phosphorus oxide ($y = n(\mathrm{Me}_{2/v}\mathrm{O})/n(\mathrm{P_2O_5})$). In the case of the $(CaO)_{0.5}(P_2O_5)_{0.5}$ sample $\mathrm{M_{NBO}} = 4$, whereas for the $(Na_2O)_{0.5}(P_2O_5)_{0.5}$ sample $\mathrm{M_{NBO}} = 2$. Given that the cations need to be associated with the NBOs for charge balancing purposes, we can use the $\mathrm{M_{NBO}}$ ratios in conjunction with the Me–O coordination number derived from the neutron data to predict how the cations coordinate with the NBOs. In the case of the $(CaO)_{0.5}(P_2O_5)_{0.5}$ glass, the Ca–O coordination number is ∼5 and there are four NBOs available for each Ca^{2+}. This means that only a quarter of the NBOs need to be coordinated to two Ca^{2+} ions and that most of the Ca^{2+} ions can be present in isolated CaO_x polyhedra. This is not the case for the $(Na_2O)_{0.5}(P_2O_5)_{0.5}$ glass where there are only two NBOs per Na^+ ion and the Na–O coordination number is ∼4. The result of this is that each NBO must be shared by two Na^+ ions and the NaO_x polyhedra must share edges leading to a Na–Na correlation across these edges. Experimentally it was found the data from the $(Na_2O)_{0.5}(P_2O_5)_{0.5}$ glass could not be satisfactorily fitted without the inclusion of a Me–Me correlation whereas this was not the case for the other datasets. Thus, it seems that the experimental results confirm the arrangement of NaO_x polyhedra predicted on the basis of the glass composition.

Previous Raman spectroscopy studies on phosphate glasses have suggested that the covalency of the Me–NBO bond increases as the field strength of the modifier cation increases [11, 12]. The results in table 1 show that the splitting of the P–O peak is greater in the data from the $(Na_2O)_{0.5}(P_2O_5)_{0.5}$ sample than in that from the two calcium containing glasses. Although, the change in bond lengths is only small, −0.01 Å for the P–NBO bond and +0.01 Å for the P–BO bond, the effect can clearly be observed in the pair distribution functions shown in figures 1–3. This provides evidence of increasing covalency in the Me–NBO bond with increasing field strength of the cation ($Ca^{2+} > Na^+$) as electron density moves away from the non-bridging oxygen to the Me–NBO bond causing the P–NBO bond to lengthen and the P–BO bond to shorten. This change in the nature of the P–NBO–Me and P–BO bonding interactions is further evidenced by the NMR spectra which exhibit a change in the Q^2 chemical shift from −19.8 to −27.4 ppm as the modifier cation changes from Na^+ to Ca^{2+}. As the Na^+ ions are replaced by Ca^{2+}, and the P–NBO and P–BO bond lengths become more similar with less localized electron density on the NBO, the environment of phosphorus becomes more similar to that in a Q^3 unit (i.e. surrounded by three equivalent oxygens). Since the chemical shift of phosphorus in a Q^3 unit is −40 ppm [13], it is expected that the Q^2 chemical shift will become more negative as the oxygens in the PO_4^{3-} group become more equivalent.

We can apply the structural information discussed above to understand better the properties of the high Ca content $(CaO)_{0.4}(Na_2O)_{0.1}(P_2O_5)_{0.5}$ biocompatible glass. We have shown that glasses of this general composition have structures comprising of Q^2 phosphate chains linked together by modifying cations. Such a structure is compatible with fibre drawing: previous work on the $CaO–Na_2O–P_2O_5$ system has shown that fibres cannot be drawn from glasses containing less than 50 mol% P_2O_5 due to the presence of a significant amount of Q^1 species [14]. In fact, a 2D rotor-synchronized ^{31}P NMR MAS study of an extruded calcium metaphosphate glass by Jäger *et al* showed clear ordering of the Q^2 chains [15]. Studies on the dissolution properties of $CaO–Na_2O–P_2O_5$ glasses have shown that the solubility decreases as the calcium content increases [2]. This can be explained in terms of the reduction in ionicity in the Me–NBO bond as the field strength of the cation is increased ($Ca^{2+} > Na^+$).

6. Conclusions

High quality neutron diffraction data collected over a wide range of Q (up to 60 $Å^{-1}$) have provided high enough real-space resolution to separate and fit the P–BO and P–NBO correlations. The results show that as the field strength of the cation increases $Na^+ \rightarrow Ca^{2+}$, the P–BO and P–NBO distances move closer together, suggesting an increase in covalency in the Me–NBO bonding. This conclusion is supported by the ^{31}P NMR data which exhibit a change in the chemical shift of the Q^2 phosphorus atoms as the Na^+ ions are replaced by Ca^{2+}.

There is another clear structural difference between the glasses containing Na_2O and CaO which relates to the connectivity of the MeO_x polyhedra. In the $(CaO)_{0.5}(P_2O_5)_{0.5}$ glass most of the Ca^{2+} ions are present in isolated CaO_x polyhedra whereas in the $(Na_2O)_{0.5}(P_2O_5)_{0.5}$ glass the NaO_x polyhedra share edges leading to a Na–Na correlation.

The high Ca containing $(CaO)_{0.4}(Na_2O)_{0.1}(P_2O_5)_{0.5}$ glass, which has potential for use in biomedical applications, is structurally similar to the $(CaO)_{0.5}(P_2O_5)_{0.5}$ glass. It is proposed that the increase in covalency in the Me–NBO bond as the field strength of the cation is increased ($Ca^{2+} > Na^+$) is responsible for the reduction in solubility of $CaO–Na_2O–P_2O_5$ glasses with increasing calcium content.

Acknowledgments

The authors wish to acknowledge funding from the Engineering and Physical Sciences Research Council (EP/C000714, EP/C000633 and GR/T21080). We thank A C Hannon of the Council for the Central Laboratory of the Research Council's Rutherford Appleton Laboratory for his help in running GEM.

References

[1] Knowles J C 2003 *J. Mater. Chem.* **13** 2395
[2] Ahmed I, Lewis M, Olsen I and Knowles J C 2004 *Biomaterials* **25** 491
[3] Bitar M, Salih V, Mudera V, Knowles J C and Lewis M P 2004 *Biomaterials* **25** 2283
[4] Ahmed I, Collins C A, Lewis M, Olsen I and Knowles J C 2004 *Biomaterials* **25** 3223
[5] Brow R K 2000 *J. Non-Cryst. Solids* **263/264** 1
[6] Hannon A C 2005 *Nucl. Instrum. Methods* A **551** 88
[7] Gaskell P H 1991 *Glasses and Amorphous Materials* (*Materials Science and Technology* vol 9) ed J Zarzycki (Weinheim: VCH) p 175
[8] Hoppe U, Walter G, Kranold R and Stachel D 1998 *Z. Naturf.* a **53** 93
[9] Witter R, Hartmann P, Vogel J and Jäger C 1998 *Solid State Nucl. Magn. Reson.* **13** 189
[10] Hoppe U, Walter G, Kranold R and Stachel D 2000 *J. Non-Cryst. Solids* **263/264** 29
[11] Matic A and Börjesson L 1998 *Phil. Mag.* B **77** 357
[12] Swenson J, Matic A, Brodin A, Börjesson L and Howells W S 1998 *Phys. Rev.* B **58** 11331
[13] Sato R K, Kirkpatrick R J and Brow R K 1992 *J. Non-Cryst. Solids* **143** 257
[14] Ahmed I, Lewis M, Olsen I and Knowles J C 2004 *Biomaterials* **25** 501
[15] Jäger C, Hartmann P, Witter R and Braun M 2000 *J. Non-Cryst. Solids* **263/264** 61